Experimental, Analytical, and Numerical Investigation of Interphasial Stress and Strain Fields in MWCNT Polymer Composites

G. C. Papanicolaou,[1] E. D. Drakopoulos,[1] N. K. Anifantis,[1] K. P. Papaefthymiou,[1] D. V. Portan[2]

[1]*Department of Mechanical and Aeronautical Engineering, Composite Materials Group, University of Patras, Patras 26500, Greece*
[2]*Department of Applied Chemistry and Materials Science, University Politehnica, Bucharest, Romania*

Received 23 December 2010; accepted 8 March 2011
DOI 10.1002/app.34498
Published online 2 August 2011 in Wiley Online Library (wileyonlinelibrary.com).

ABSTRACT: In this investigation, the effect of polymer matrix-MWCNT interphase on the stress and strain fields developed at the close vicinity of MWCNT was studied. The recently developed concept of the hybrid interphase (Papanicolaou et al., 2002) was applied. According to this concept, the interphase thickness depends on the property considered at the time. The parameter of imperfect bonding between the primary constituent materials is also introduced by means of the degree of adhesion. Experimental findings combined with analytical and numerical results gave a better understanding of the structural and mechanical performance of epoxy resin-carbon nanotubes composites. © 2011 Wiley Periodicals, Inc. J Appl Polym Sci 123: 699–706, 2012

Key words: nanocomposites; modeling; interfaces; carbon nanotubes; finite element analysis

INTRODUCTION

Nanocomposites constitute a very special category of composite materials. Nanoparticles exhibit properties that are significantly different from the bulk material. The reason is that phenomena that are negligible at large scales cannot be ignored at the nanoscale. Moreover, due to large fraction of surface area, only a small amount of nano-inclusions is adequate for the nanocomposite to achieve unique mechanical, electrical and other properties. Especially during the last decade, carbon nanotubes have attracted the attention of the scientific community due to their unique behavior. Carbon nanotubes were firstly reported by the Russians Lukyanovich, V.M. and Radushkevich, L.V in 1952[1] but no further investigation took place because of the lack of knowledge to massive production. After an extended research by Iijima, S. in 1991[2] carbon nanotubes became a new attractive material to Nanotechnology.

At present, an extended research activity related with carbon nanotubes reinforced polymer composites and other possible applications of CNT's is being carried out in an effort to exploit their unique behavior. It is worth to mention some of the exceptional mechanical properties of the nanotubes; the axial Young's modulus, and the elongation to break of a SWCNT have been computed in the range of 0.9-1.3 TPa and 30-40% respectively.[3–8] Nonetheless, it has been proved rather perplex to manufacture nanocomposites with the desired properties. To a large extent, one of the problems encountered is the inclusions' tendency to agglomerate resulting in a composite with micro-structure instead of a nano-structure. The dispersion of nanotubes in the matrix can be enhanced through physical-mechanical or chemical[9] processes. Physical methods involve breaking up the agglomerates through impact (ball milling), shear (high speed shearing), and oscillation at high frequency (ultra-sonication) or a combination of them. Concerning the chemical methods, purification procedure is twofold[10] (1): to remove the metallic catalyst residues, which arise from CNT synthesis and (2) to create functional groups on the surface or caps of the CNTs. These functional groups are the reactive sites of the CNT surfaces during further chemical modifications. They can also improve the polymer-CNT interfacial interactions. Therefore, results from TGA analysis[11] report a compromise between the functionalisation parameters (sonication, concentration of acid treatment etc) and damage of the graphitic structure of CNT's.

In this work, multiwalled carbon nano-tubes (MWCNT)—epoxy nanocomposites were manufactured and mechanically characterized. Five different

Correspondence to: G. C. Papanicolaou (gpapan@mech.upatras.gr).

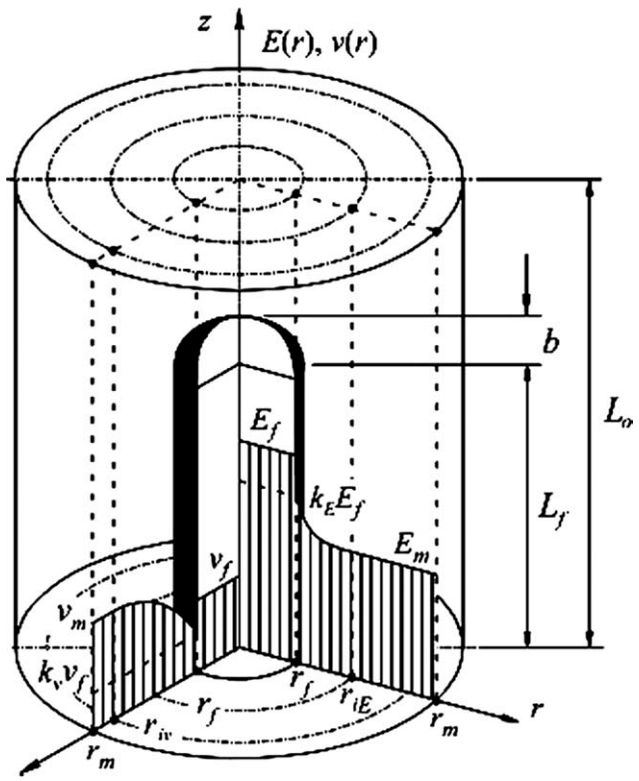

Figure 1 RVE along with the hybrid interphase concept.

filler volume fractions were applied by implementing a high speed shearing technique. Subsequently, a theoretical investigation of the MWCNT—matrix interphase region involving the hybrid interphase concept was conducted, in an effort to study both analytically and numerically its effect on the interfacial stress field developed in the area close to MWCNT's.

THE HYBRID INTERPHASE CONCEPT

A key factor for the overall performance of micro and nanocomposites is the polymer-reinforcement interphase which is a third phase created during manufacturing in the area immediately surrounding the fibers, having properties and microstructure different from those of the two main constituents of the composite. The interphase formed during manufacturing of the composite is the so-called structural interphase.[12,13] Within this region a rather complex situation is developed involving areas of imperfect bonding, where mechanical stresses and stress singularities are developed due to the filler's geometry and the constraint imposed to the matrix deformation. This, finally results in the creation of microcracks, voids, and other discontinuities. The structural interphase can be observed by means of microscopy and must be distinguished from the hybrid interphase. More precisely, by the term "hybrid interphase" it is meant the interphase material having a volume fraction which corresponds to the percentage of the bulk matrix surrounding the reinforcement in which a specific matrix property is strongly affected by the existence of the reinforcement, whereas the hybrid interphase thickness represents the maximum radial distance from the inclusion boundary in which this property is affected by the inclusion's presence. This denotes that the interphase is not simply a geometrical concept; dependent only on the volumetric composition of the composite, but it is mainly a property-dependent concept.[12–14] Recent investigations have proved the validity of the above conception.[14–17]

Theoretical background

The micromechanical modeling of the hybrid interphase region requires several assumptions to be made. Some basic assumptions, regarding the material properties are: (i) A linear elastic behavior of all phases is assumed; (ii) the fibers are transversely isotropic; (iii) The global composite behavior can be modeled by a representative volume element, RVE (Fig. 1).

The concept of the hybrid interphase is based on two main assumptions. The first one considers a nonhomogeneous interphase whose material properties depend on the respective properties of a homogeneous fiber and matrix material, with a thickness depending on the volumetric composition of the composite.[18] The second assumption introduces imperfect adhesion between fiber and matrix materials by appropriate definition of material's properties. It is apparent that perfect bonding between fiber and matrix does not exist in reality due to the existence of flaws, fiber surface roughness, and other physical and mechanical interactions. This imperfection is described by the adhesion efficiency coefficient which represents the discontinuity of a property at the fiber-matrix interface:

$$k_E = \frac{E_i(r_f^+)}{E_f},\ k_\nu = \frac{\nu_i(r_f^+)}{\nu_f} \tag{1}$$

where E, ν, r represent the elastic modulus, Poisson's ratio and radius and the subscrips i, f stand for fiber and interphase, respectively. Thus, the value of a property at the fiber-matrix boundary, with regard to eq. (1) becomes

$$E_i(r = r_f^+) = k_E E_f \qquad \nu_i(r = r_f^+) = k_\nu \nu_f \tag{2}$$

As shown in a recent by the author's investigation,[13] the main factors affecting the interphase

TABLE I
Epoxy Resin's and Carbon Nanotubes' Mechanical Properties of Elasticity

E_{matrix}		E_{f11}	E_{f22}	E_{f12}	E_{f23}		
GPa	ν_{matrix}	GPa	GPa	GPa	GPa	ν_{f12}	ν_{f23}
3.08[a]	0.3[a]	704[b]	345.54[b]	227.04[b]	125.52[b]	0.14[b]	0.3764[b]

[a] Experimentally determined.
[b] Seidel et al.[23]

thickness are: the adhesion coefficient, k, the reinforcement radius r_f and the material's anisotropy coefficient, S. Then, the property-dependent hybrid interphase thickness is given as:

$$t_E = S_E \cdot r_f \cdot \frac{1-k_E}{k_E} \quad t_\nu = S_\nu \cdot r_f \cdot \frac{1-k_\nu}{k_\nu} \tag{3}$$

where

$$S_E = E_T/E_L, \qquad S_\nu = \nu_T/\nu_L \tag{4}$$

are the anisotropy indices of the RVE. The subscripts T, L denote the principal values of property along the transverse and longitudinal directions, respectively. Considering perfect fiber-matrix adhesion, homogeneous fiber distribution, perfectly linear elastic behavior and unidirectional fiber orientation, then the well-known relations can be obtained:

$$E_L = E_f\upsilon_f + E_m(1-\upsilon_f) \quad E_T = \frac{E_f E_m}{E_f(1-\upsilon_f) + E_m\upsilon_f} \tag{5}$$

$$\nu_L = \nu_f\upsilon_f + \nu_m(1-\upsilon_f) \quad \nu_T = \frac{\nu_f \nu_m}{\nu_f(1-\upsilon_f) + \nu_m\upsilon_f} \tag{6}$$

where υ_f represents the filler volume fraction and the indice m corresponds to the matrix material. However, considering imperfect adhesion conditions, the effective fiber volume fraction based on the property considered can be modified as:

$$\upsilon_{fE} = k_E\upsilon_f, \qquad \upsilon_{f\nu} = k_\nu\upsilon_f \tag{7}$$

So now, k_E and k_ν can be expressed as:

$$k_E = \frac{E_c - E_m}{E_f - E_m}\frac{1}{\upsilon_f} \quad \text{or} \quad k_E = \frac{E_f}{E_T}\frac{E_T - E_m}{E_f - E_m}\frac{1}{\upsilon_f} \tag{8}$$

$$k_\nu = \frac{\nu_c - \nu_m}{\nu_f - \nu_m}\frac{1}{\upsilon_f} \quad \text{or} \quad k_\nu = \frac{\nu_f}{\nu_T}\frac{\nu_T - \nu_m}{\nu_f - \nu_m}\frac{1}{\upsilon_f} \tag{9}$$

As shown in previous publications,[12,13] the interphase stiffness and Poisson's ratio variation within the interphase region in the radial direction is given by:

$$E_i(r) = E_m + (k_E E_f - E_m)\exp\left\{-\frac{k_E}{1-k_E}\frac{1}{S_E}\frac{r-r_f}{r_f}\right\} \quad r_f \le r \le r_{iE} \tag{10}$$

$$\nu_i(r) = \nu_m + (k_\nu \nu_f - \nu_m)\exp\left\{-\frac{k_\nu}{1-k_\nu}\frac{1}{S_\nu}\frac{r-r_f}{r_f}\right\} \quad r_f \le r \le r_{i\nu} \tag{11}$$

where r_{iE}, $r_{i\nu}$ represent outer interphase boundaries.

NUMERICAL ANALYSIS

Geometric complexity and material inhomogeneities of the RVE impose a demand for a numerical determination of the interphasial stress field. In this study, finite element procedures have been utilized to study the response of a FRP (fiber reinforced polymer) incorporating a hybrid interphase region. The geometry of the model used is shown in Figure 1 and requires axisymmetric analysis associated with appropriate material inhomogeneities.

In the proposed model, it was assumed that a fiber with the elastic properties shown in Table I can simulate a MWCNT. In addition, it was assumed that the fiber has a constant radius, $r_f = 13$ nm and a half-length, $L_f = 15.38\ r_f$, while the fiber volume fraction is a global independent variable. The fiber is surrounded by the hybrid interphase, the properties of which are varied with radial distance according to eqs. (10)–(11). These two analytic equations were used as input data for the interphase material properties of the finite element model applied. Figures 2 and 3 depict the corresponding finite element model for a volume fraction $\upsilon_f = 0.25\%$ ($w_f = 0.3\%$). The mesh refinement in the regions where high material degradation or high stress concentration is expected (i.e., at the exact fiber-interphase boarder) to occur is apparent. Table II shows the size of the finite element model.

MATERIALS AND METHODS

Materials

A diglycidyl ether bisphenol A (DGEBA)-based epoxy system (31185 D.E.R.™ 332) was used as matrix along with a curing agent type 132098 based on TETA (triethylene tetramine), both provided by SIGMA-ALDRICH®, reinforced with Nanothinx S.A.© NTX1 MWNT's. The properties of raw nanotubes according to manufacturer's data sheet can be observed in Table III.

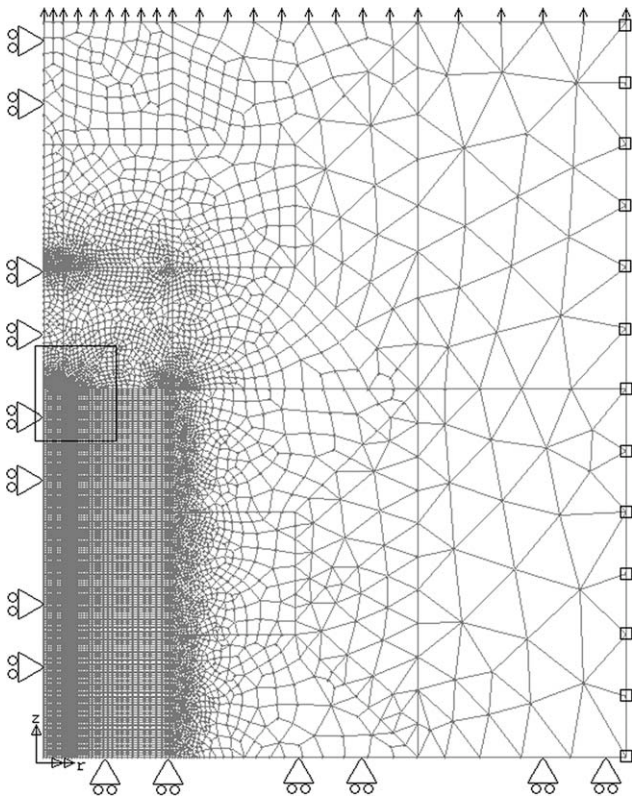

Figure 2 Typical finite element model corresponding to a flat fiber tip.

Manufacturing procedure

High speed shearing was utilized to disperse the nanotubes in the resin at controlled conditions of pressure, temperature and speed using a high speed dissolver type Dispermat AE, VMA Getzmann GmbH. After several preliminary tests, for achieving a homogeneous dispersion, the process was finally optimized as follows: nanotubes were mixed with the resin in the dissolver for 2 h under vacuum at 2300 rpm and 50°C. Next, the hardener was added at a ratio of 14 P.H.R. while mixing procedure was continued. Finally, the mixture was put into special molds having the exact dimensions of the three point bending specimens to be used. The material was then cured for 24 h at 80°C. The fiber loadings applied were 0%, 0.3%, 0.7%, 1%, 2%, and 3% w_f in MWCNT's. The specimens' dimensions were 100 mm × 12.8 mm × 2.2 mm (±0.2 mm) and the span between the grips was fixed at 63 mm. All bending tests were performed at room temperature using an INSTRON 4301 universal testing machine with a constant displacement rate of 1 mm/min.

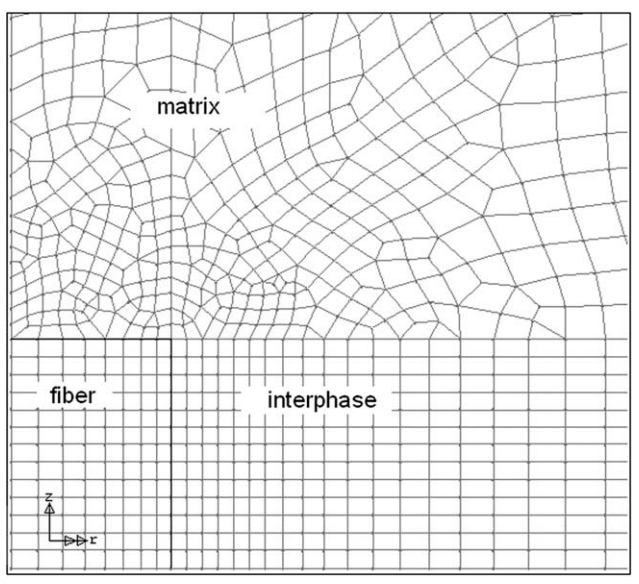

Figure 3 Magnified area for better resolution of the mesh on the boundaries.

TABLE II
Size of Axisymmetric Finite Element Model

Linear elements	Nodes	Fiber radius	Fiber length	RVE radius	RVE length
10,891	10,779	13 nm	200 nm	316 nm	400 nm

RESULTS AND DISCUSSION

Characterization of mechanical response

The exact values for the flexural modulus as a function of w_f (%) are presented in Figure 4. From these figures, one can observe that specimens reinforced with 2% w_f showed a degradation in modulus when compared with the matrix modulus while, in contrast, specimens reinforced with 0.3, 0.7, 1 and 3% w_f with CNT's showed a relative increase in modulus. A significant change of 10.6% and 14.03% was measured for 0.3% w_f and 3% w_f respectively. In addition, as shown in Figures 5 and 6, a general reduction in both flexural strength and failure strain was observed. The higher the CNT weight fraction is, the more brittle the nanocomposite becomes. This type of mechanical behavior can be attributed to more than one reason. Two competing phenomena that

TABLE III
Properties of Raw Carbon Nanotubes

NTX1 MWNT's		Characterisation method
Synthesis method	CVD	
Form	Black powder	
Diameter	15–35 nm	TEM,SEM
Length	≥10 μm	TEM,SEM
Number of walls	15–35	TEM
Purity	97%	TGA,SEM
Metal particles	3%	TGA
Amorphous carbon	<1%	TGA,Raman
Surface area	200–250 m^2/g	BET
Bulk density	≈0,16 g/cm^3	

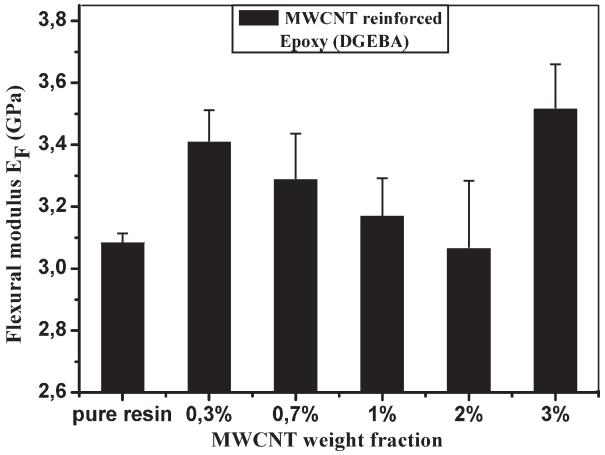

Figure 4 Flexural modulus variation for different fiber loadings.

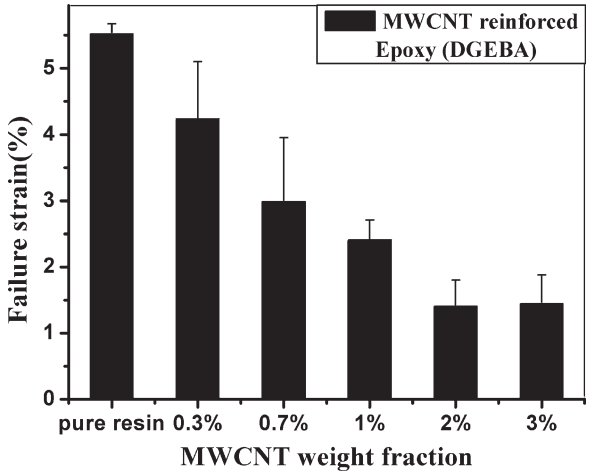

Figure 6 Failure strain variation for different fiber loadings.

have inverse effect upon the material's response, the adhesion and agglomeration, are among the principal mechanisms that affect the behavior of the composite. Concerning the modulus of elasticity (Fig. 4), at low weight fractions, where the agglomeration of filler particles is small, the effect of adhesion dominates and, consequently, a macroscopic increase of the modulus can be observed. As the quantity of nanotubes in the matrix increases, so does the degree of agglomeration. Voids, microcracks, deficient wetting of the filler etc are phenomena that become more intense and dominate upon the increasing of stiffness that is introduced by the addition of nanotubes and the modulus of the composite material reaches a minimum value at $w_f = 2\%$. However, for further increase in the MWCNT's weight fraction, an increase in the modulus of the material is inevitable, due to their outstandingly high stiffness. Besides the two aforementioned principal factors, there are numerous additional parameters that should be taken into account to obtain a broader perception of the reasons for such a behavior (Fig. 4). In a composite with high filler volume fraction, one may deduce two possible microstructures in addition to that where particles are randomly dispersed. In the first case, the resin is completely entrapped within the filler aggregates or clusters, with fillers touching each other. In the second type of microstructure, the composite contains a combination of regions of resin entrapped within filler clusters. In principal, such composites would consist of regions with randomly dispersed fillers, but with each region containing a different volume fraction.[20]

In regard to the flexural strength (Fig. 5), the reinforcing potential of MWCNT's is undermined by the effect of agglomeration. At low weight fractions, where the agglomerates are smaller, resulting in higher surface area, loads can be transferred to the nanotubes, resulting in a considerable increase of the ultimate strength. By increasing the filler's weight fraction the degree of agglomeration causes a brittle behavior which can be attributed to the following reasons: Reduced surface area results in inefficient load transfer from matrix to nanotubes, while agglomerates, voids, microcracks, and other discontinuities act as points of local stress concentrations. The degradation of the material's failure strain (Fig. 6) is also attributed to the same phenomena.

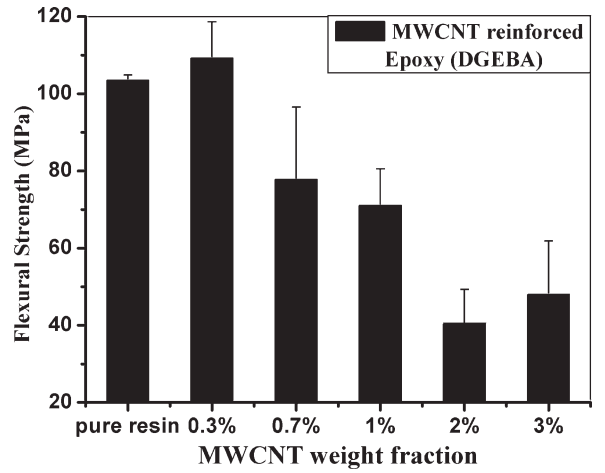

Figure 5 Flexural strength variation for different fiber loadings.

Application of the hybrid interphase model

The variation of the elastic modulus and the Poisson's ratio within the hybrid interphase area are being illustrated in Figure 7. As it can be observed, the hybrid interphase thickness has a different extent with respect to each one of the properties under consideration. The effect of the degree of adhesion upon the abrupt variation of a property value observed at the fiber–matrix border is, also, apparent.

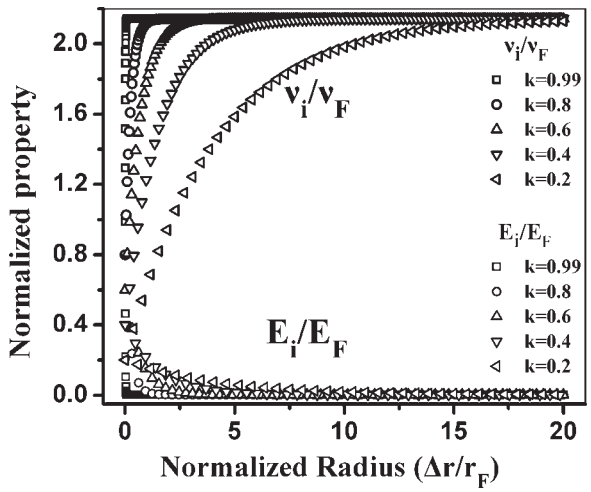

Figure 7 Elastic material property variation within the hybrid interphase area for different degrees of adhesion.

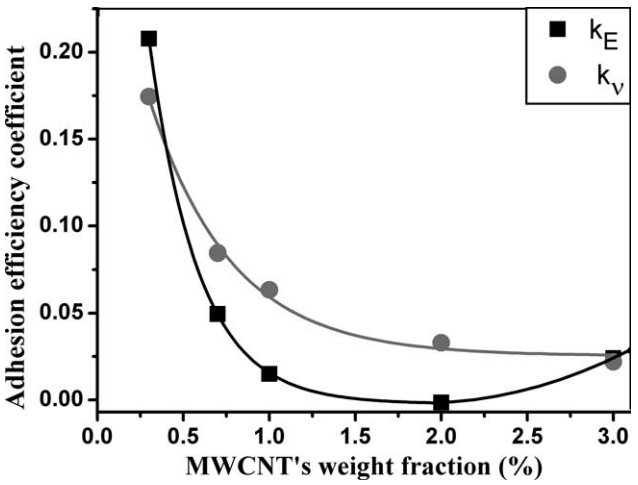

Figure 9 Adhesion efficiency coefficient as a function of w_f in MWCNT's.

Additionally, the distribution of the stress–strain field along the interphase is also affected by the fiber–matrix degree of adhesion. It should be stressed that the adhesion coefficient, k, represents the discontinuity at the filler–matrix boundary. The magnitude of this discontinuity is not the same for all the properties. This is confirmed by the dependence of hybrid interphase thickness upon the property considered each time (Fig. 9). Moreover, a divergence of 100% between the values of the hybrid interphase thickness with respect to the two considered properties is observed (Fig. 8). As it can, be observed the interphase thickness is higher when approached by means of interphase stiffness rather than the Poisson's ratio. This confirms the property dependent nature of the hybrid interphase and is attributed to the vast difference between CNT and matrix modulus, however, as perfect adhesion conditions are approached the hybrid interphase thickness tends to zero. The variation of k_E, k_v as a function of filler's weight fraction can be observed in Figure 9. A general fall in the degree of adhesion is attributed to increased agglomeration, a mechanism that is extensively discussed in section Characterization of mechanical response. It should be noted that a similar behavior, expressed by means of reinforcement efficiency of CNT's, was observed by Martone et al.[21] The fiber–matrix adhesion efficiency coefficient, with respect of the Elastic Modulus and the Poisson's ratio, for the nanocomposites studied in this work was found to be equal to 0.207 (eq. 3) and 0.174 for $w_f = 0.3\%$, respectively. For the given values of these coefficients, the interphase regions of two successive fibers overlap to each other rendering the matrix material a modified material having properties completely different from the bulk, for the specific fiber volume fraction. At higher volume fractions, where the distance between two successive fibers is smaller it is obvious that the matrix will be completely transformed, as well.

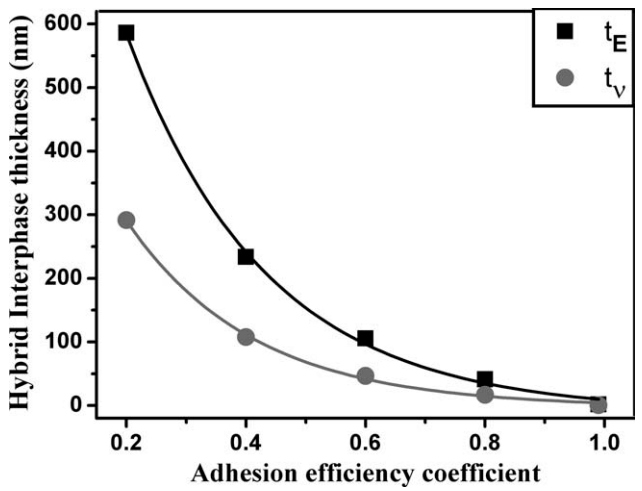

Figure 8 Interphase thickness of hybrid interphase with respect to the elastic modulus and Poisson's ratio as a function of the adhesion efficiency coefficient.

Numerical Results

To study the effect of the interphase existence in MWCNT-Epoxy resin nanocomposites, the above-developed hybrid interphase model has been utilized in finite element procedures. The stress field in the interphasial area, according to the model shown in Figure 2, for imperfect adhesion conditions is presented in Figures 10–13. More precisely, according to Figures 10-11 the normal and shear stresses developed at the radial direction are highly dependent on the degree of fiber–matrix adhesion. Normal stresses were calculated at the center and shear stresses at a distance of 5 nm from the tip of the nanotube bearing in mind that the maximum values of the stresses

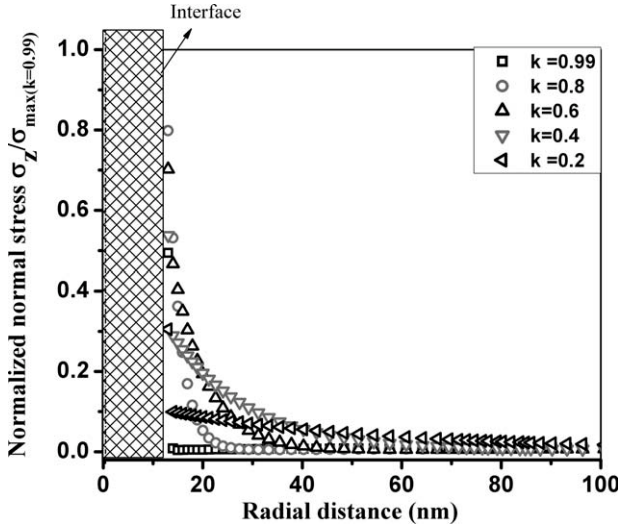

Figure 10 Normalized normal stresses in the radial axis for various adhesion coefficients.

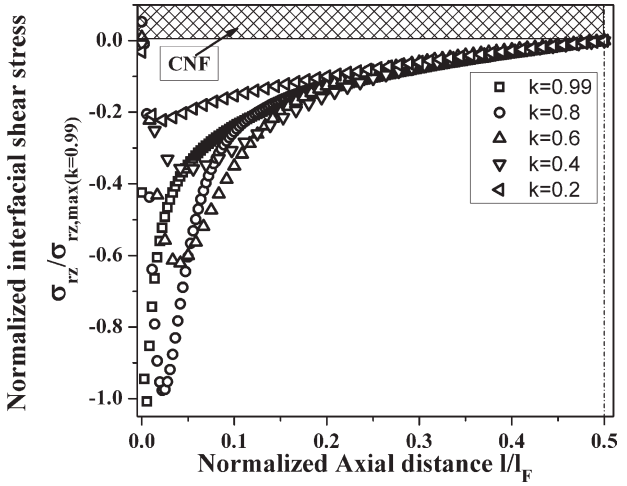

Figure 12 Normalized interfacial shear stresses developed for various adhesion coefficients.

can be observed at these points, respectively. At higher values of k there can be observed an increase at the stresses developed at the vicinity of nanotube which implies that the reinforcement takes up a greater amount of loads as it is meant to do. Also, the small extent of the region, where increased stress is observed, implies a narrow interphase region. Moreover, the effect of adhesion efficiency coefficient upon the shear lag phenomenon is observed in Figure 12. More precisely, for lower values of adhesion efficiency coefficient an inefficient load transfer from the matrix to the fiber leads to the development of lower the interfacial shear stress at the fiber tips. This might appear to be desirable. However, since the applied loads are transferred from the matrix to the fiber through shear, lower shear stresses at the interphase would lead to lower normal stresses at the fiber. Consequently, since a smaller portion of the external loads is taken up by the reinforcement, this would result in not taking full advantage of its high strength, but on the contrary over encumbering the weaker matrix. As a result, lower values of adhesion efficiency coefficient mean inefficiently loading the reinforcement and premature failure of the matrix. It should be noted that the stress field is known to be sensitive to the fiber tip shape as investigated and confirmed in a previous publication by the authors.[13] Finally, a theoretical model for the computation of the normal and shear stress distribution along the fiber length at the fiber-matrix interface developed in a previous publication by Papanicolaou et al.[22] was applied and analytical results were compared with respective values derived by means of the finite element model described above. The agreement between the FEM results and the respective ones derived by the analytical model, as presented in Figure 13, is almost

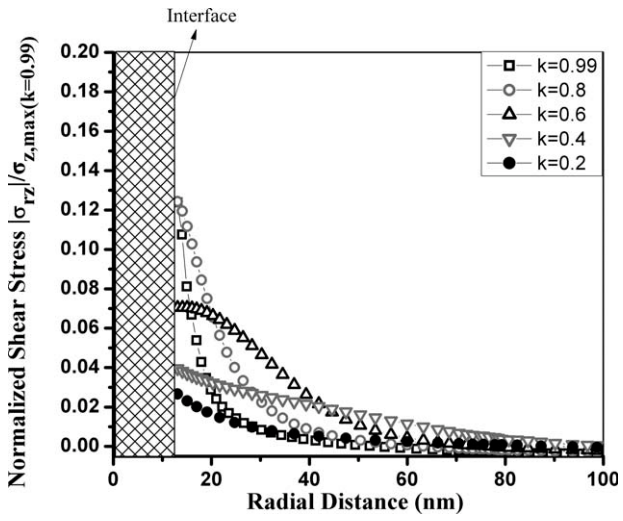

Figure 11 Normalized shear stresses in the radial axis for various adhesion coefficients.

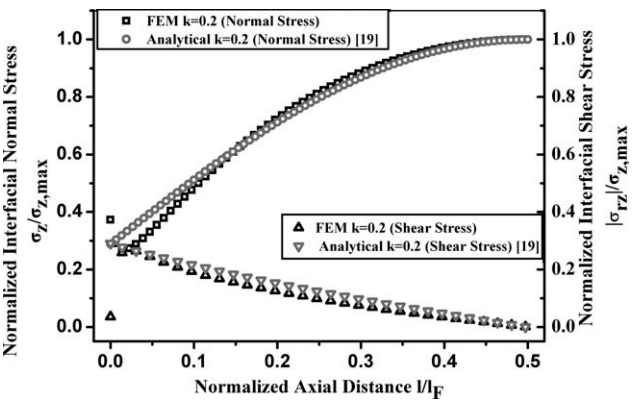

Figure 13 Comparison between analytical and numerical results for the normalized interfacial normal and shear stress.

perfect and this is because the analytical model is taking into account the adhesion coefficient "*k*" as well as the interface stiffness "*K*" which is a measure of the stiffness of the fiber–matrix boundary measured in GPa and which, in turn, depends upon the fiber–matrix adhesion coefficient, "*k*," as well.[19]

CONCLUSIONS

In the present study a series of MWCNT-resin materials with different fiber volume fractions were manufactured and mechanically characterized. The material's mechanical behavior is governed by more than one phenomena, two of which are the degree of adhesion between the constituent materials and the agglomeration of the particles in the matrix. Experimental results implied imperfect adhesion conditions between matrix and CNT's. The interphase regions of two successive nanotubes overlap each other, yielding a matrix material with different properties from the bulk. Next, the hybrid interphase model was applied to evaluate the interphasial fiber–matrix stress field. The adhesion coefficient, *k*, was introduced, as a measure of the imperfect bonding of the constituent phases which represents the discontinuity of a property at the filler–matrix boundary. This discontinuity is not the same for every property considered. Adhesion efficiency was also found to decrease at higher filler weight fractions. This is attributed to a more intense agglomeration of CNT's, which also rendered a macroscopically brittle behavior. Also a significant influence of the property considered upon the hybrid interphase thickness was observed, which confirms its property dependent nature.

Analytical investigation was combined with FE-analysis of normal and shear stress fields that were developed at the fiber-CNT interface and at a direction normal to it. Results were found to be sensitive to the radial distance from the fiber and also to the degree of adhesion between the fiber and the matrix. It can be inferred that higher values of *k* would be desirable, since the loads are more efficiently transferred from matrix to reinforcement. However, in such case, the interfacial stress concentrations are magnified which is a possible mechanism of failure initiation. Finally, a comparison of numerical with analytical results gave satisfactory convergence which is due to adopting a realistic approach.

References

1. Rykov, V. T.; Lukyanovich V. M.; Radushkevich L. V. Bull Acad Sci USSR Div Chem Science 1952, 1, 395.
2. Iijima, S. Nature 1991, 354, 56.
3. Giannopoulos, G. I.; Kakavas, P. A.; Anifantis, N. K. Comp Mater Sci 2008, 41, 561.
4. Yakobson B. I.; Smalley, R. E. 1997, 85, 324.
5. Salvetat-Delmotte, J.-P.; Rubio, A. Carbon 2002, 40, 1729.
6. Yakobson, B. I.; Campbell, M. P.; Brabec, C. J.; Bernholc, J. Comp Mater Sci 1997, 8, 341.
7. Wang, Z. L.; Gao, R. P.; Poncharal, P.; de Heer, W. A.; Dai, Z. R.; Pan, Z. W. Mater Sci of Eng C 2001, 16, 3.
8. Fisher, F. T.; Bradshaw, R. D.; Brinson, L. C. Comp Sci Tech 2003, 63, 1689.
9. Spitalsky, Z.; Tasis, D.; Papagelisb, K.; Galiotis C. Prog Polym Sci 2010, 35, 357.
10. Sertan, Y.; Goknur, B. JAPS 2011, 119, 3360.
11. Aviles, F.; Cauich-Rodriguez, J. V.; Moo-Tah, L.; May-Pat, A.; Vargas-Coronado, R. Carbon 2009, 47, 2970.
12. Papanicolaou, G. C.; Michalopoulou, M. V.; Anifantis, N. K. Comp Sci Tech 2002, 62, 1881.
13. Papanicolaou, G. C.; Anifantis, N. K.; Keppas, L. K.; Kosmidou, T. V. Comp Interf 2007, 14, 131.
14. Pompe, G.; Mäder, E. Comp Sci Tech 2000, 60, 2159.
15. Jayaraman, K.; Reifsnider, K. L.; Swain, R. E. J Comp Tech Res 1993, 15, 4.
16. Chouchaoui, C. S.; Benzeggah, M. L. Comp Sci Tech 1997, 57, 617.
17. Kim, J. K.; Sham, M. L.; Wu, J. Comp A 2001, 32, 607.
18. Lipatov, Y. S. International Pol Sci Tech Monograph 1977, 2.
19. Kakavas, P. A.; Anifantis, N. K.; Baxevanakis, K.; Katsareas, D. E.; Papanicolaou, G. C. J Mater Sci 1995, 30, 4541.
20. Wu, W.; Sadeghipour, K.; Boberick, K.; Baran, G. Mater Sci Eng A 2002, 332, 362.
21. Martone, A.; Formicola, C.; Giordano M.; Zarrell, M. Comp Sci Tech 2010, 70, 1154.
22. Papanicolaou, G. C.; Bakos, D. J.; Kosmidou, T. V. Comp A 2007, 38, 1099.
23. Seidel, G. D.; Hammerand, D. C.; Lagoudas, D. C. Sandia Report 2007, Unlimited Release.